An Approach to Motor Control for Spike-based Neuromorphic Robotics

Fernando Perez-Peña
Applied Robotics Lab,
School of Engineering
University of Cadiz, Spain
fernandoperez.pena@uca.es

Alejandro Linares-Barranco
Robotic and Technology of Computers Lab
School of Computer Engineering
University of Seville, Spain

Elisabetta Chicca
Cognitive Interaction Technology, Center of Excellence (CITEC)
Faculty of Technology
Bielefeld University, Germany

***Abstract*—This paper presents an approach to open-loop motor control using Integrate and Fire (IF) neurons. The controller aims at mimicking motor control structures found in the brain and consists of three neuron populations implemented on different VLSI chips. The first population codes the distance to the target in a form of a firing rate (similarly to some class of cells found in Area 4 in the motor mammalian cortex). The second population mimics the behavior of neurons of the basal ganglia and control the gating and speed of the movement, by means of an NMDA synapse and an excitatory connection. The third population codes the supposed position reached by the robot. The multi-chip neuromorphic setup is interfaced with a Field-Programmable Gate Array (FPGA) board by the Address Event Representation (AER) communication protocol. The FPGA elongates the spike duration to make them suitable for driving the motors with Pulse Frequency Modulation (PFM). This approach aims to compete with classic controllers offering lower power, simplified control and smoother movements.**

Keywords—neuromorphic hardware, motor control, spike-based, robotics

I. INTRODUCTION

We present an algorithm for motor control implemented with neuromorphic hardware [1]. The neuromorphic engineering field aims to mimic the behavior observed in biological nervous systems. The origin of this research field dates back to the late eighties, since then the researchers have concentrated efforts in developing sensors, analog chips with a large quantity of Integrate and Fire (IF) neurons , synapses and learning circuits as well as a broad number of circuits to reproduce some specific functionality observed from *in-vivo* experiments [2]. Although the community major attention has been focused on solving specific tasks by creating new analog circuits, more recently large-scale architectures have been developed [3-5]. The currently available real-time neuromorphic systems are well suited for exploring biologically inspired motor control algorithms. Recently, a classical industrial approach such as Proportional-Integral-Derivative (PID) control has been proposed to develop a neuromorphic motor controller [6, 7]. Nevertheless, this approach is developed under industrial constrains that might not fit with neuromorphic engineering goals. Recent work presented in [8] describes the use of neuromorphic hardware to control the robot motor torques. Our research aims at developing a full motor controller closely inspired by the control mechanisms found in the human nervous system. This research has high potential for improving understanding of biological motor control, developing novel controller techniques and eventually substantially reducing power consumption. This is the first attempt to use analog low-power subthresold VLSI IF neurons for motor controlling (without using a microcontroller) and it is currently limited to open loop control. The controller proposed in this work is modeling the first layer related to movement planning [9] and it is currently being updated to implement a second layer where the loop is closed.

This work is based on the results presented in [10] for the Vector Integration To-End point (VITE) bio-inspired algorithm and its translation to the event-based processing paradigm using building blocks on a Field Programmable Gate Array (FPGA) [11]. The original algorithm was designed for calculating a non-planned trajectory. It computes the difference between a target and a present position referred to muscles' lengths by iterative calculation of the difference between the target and the present position without using any feedback: the command signal is used to estimate the current position. The a-lgorithm includes a so called GO signal which let you control the speed. A non-zero value of GO signal will trigger the movement and the speed control is encoded in its temporal profile. The shape of the signal proposed in [10] was a ramp, and its slope was used to set the speed of the movement. The main contribution of the original algorithm on its own is, so far, the generation of the position and the speed profile trajectory that the joint should follow. The goal of this research is to use the algorithm described to control a robotic arm platform under the constraints of the spiking neural networks based on IF neurons. Using a classic robotic arm, the features of the algorithm are tuned to adapt the concept of muscles to motors. So, a direct translation of the algorithm would lead to loss of functionality; we therefore included new features suitable for the spiking neurons in use. In a motor driven robotic arm two variables are crucial for the control algorithm: the target position and the current position. In the new version of the algorithm, these two variables represent the space position that the joint of the limb aim to reach. In a spiking neural network these analog variables can be represented by the frequency of neurons. We used three populations of IF neurons to encode the three variable requested by the motor control algorithm, namely the difference between the target and the reached position, the effect produced by the GO signal and the estimated position. The resulting neural network is designed to control one motor of the robot and it could be replicated to control n degrees of freedom. Given the open loop nature of the current algorithm, the descending control signal is used to estimate the present position. We plan to further extend the algorithm by using motors with encoders. The signals provided by usual encoders include the position and the velocity, so they can be used to implement a second stage where the loop is closed. This second stage will interface the first planning stage to adjust its behavior.

In this paper we describe the biological motivation and the methodology followed (Sec. II), the network model proposed (Sec. III), the results for the software (Sec. IV) and hardware implementation of the control model (Sec. V), and finally discuss current achievement and possible outlook (Sec. VI).

II. Biological Motivation and Methodology

In the late eighties Bullock and Grossberg proposed a biologically realistic model of planned arm movements [10] broadly used at the robotics field [12-14]. The model follows the principles of how intended movements are carried out by humans. This section aims to update the relation between the model proposed and the biological properties that nowadays are known. Finally, we describe the methodology to check the behavior of the new model.

Neurophysiological data supports the choice of the main computational blocks of the algorithm: in [10], some similarities with the population which codify the difference between the target position and the present position are shown. This population is called Difference Vector (DV) population and is matched with cells found in the precentral motor cortex (Area 4). In [10], also the gating mechanism involving a trigger signal is shown. This so called GO signal can be assimilated with one function of the basal ganglia (BG) in motor control [10]. The BG is the largest subcortical structure placed at the base of the forebrain. The main components are: the globus pallidus (GP), the striatum, the nucleus accumbens, the substantia nigra and subthalamic nucleus. The matched behavior is, specifically, with the activity found on the globus pallidus.

We studied the model proposed in [10] in light of more recent biological findings. Furthermore, the mapping of the original model to analog spiking neural networks forced us to include more detailed neural dynamics (e.g. NMDA) to achieve similar performances. The model can be enhanced by including further details related to the basal ganglia behavior [15-19].The experimental results presented in [15] strongly support the existence of movement gating. Nevertheless, the work presented in [16] lead to the hypothesis that the basal ganglia alone cannot account for full movement control and cortical structures must also be involved. According to [17], the initiation of muscular movements is preceded by activity in the cerebral followed by activation of the GP. This observation also supports the VITE model by thinking of a pre-computation of the difference between the target position and the present position meanwhile GO signal has a zero value. In [18], the basal ganglia role in movement generation is explained as follows: once the cortex has come to a decision of making a specific movement (stimulus is delivered), the striatum (region of the basal ganglia target of cortical input) is activated. Then, internal complex activity of the BG releases the pathways to allow the movement. In particular, direct projections from the cortex to the striatum and subthalamic nucleus are believed to activate the basal ganglia [19]. The input to the striatum is mediated by the N-methyl-D-aspartate (NMDA) receptors while the input to the subthalamic nucleus targets the non-NMDA channels. Furthermore, in [19], the authors support the idea that cortical activity is necessary to activate the BG.

The model we propose takes inspiration from these observations and incorporates the basal ganglia function and the NMDA channels role in a simplified neural network suitable for controlling a robotic platform. We simulated our model on a standard desktop using the Brian Simulator [20] to characterize the network dynamics. The simulation results guided the subsequent neuromorphic implementation using a multi-chip setup [1].

III. Network Model

A schematic drawing of the proposed neural network is shown in Fig. 1. The network comprises three different populations: the Difference Vector (DV) population encodes the difference between the target and the estimated current position; the GO population implements movement gating and speed control; the Present Position Commands (PPC) population encodes the estimated current of the robotic arm.

Four excitatory connections are part of the network: a couple of them are inputs and the other two are used to connect populations. The target stimulus (constant rate spike stream) excites all the neurons of the DV population and it is tuned to produce a one to one relation between presynaptic and postsynaptic action potentials. The GO signal stimulus excites the GO population and it is a spike stream in which the rate increases over time. Short-time depression in the synaptic connection prevents the production of post-synaptic spikes in absence of a target stimulus. Finally, we have two excitatory recurrent synapses: one to connect the DV population with the GO population (as described in the next paragraph) and the other one to connect the GO population and the PPC population to update the position by integrating the incoming spikes.

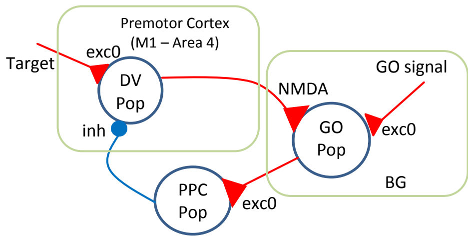

Fig. 1. Spiking neural network diagram.

The GO population has a special synapse that connects it to the DV population. This synapse plays the role of the NMDA channels described in Section II. With this synapse, the desired behavior is achieved: neither the target nor the go stimulus presynaptic spikes in an isolated way will produce any postsynaptic action potential, which results in the desired gating movement function. The NMDA synaptic circuit produces an output current only if the membrane potential of the post-synpatic neuron is above a fixed threshold, referred as NMDA threshold and set by an input bias voltage. The excitatory synapse of the GO signal will keep the membrane potential higher than the NMDA threshold but without firing. Then, when a presynaptic spike occurs in the connection with the DV population, the membrane potential is higher than the NMDA threshold thus allowing the NMDA synapse to produce an output current and trigger a spike in the postsynaptic neuron. The last connection is the inhibition between PPC and DV population. This synapse is tuned to inhibit the output firing rate of the DV population when the PPC has reached the firing rate set by the stimulus (robot has reached the target location)

IV. Simulation Results

This section presents the results obtained using the Brian simulator to verify the performance of the network described in the previous section. The simulations are done with one neuron per each population (one-to-one fashion connected). Fig. 2 shows the firing rate of each population including both stimuli: the target which excites the NMDA and the GO signal which excites the non-NMDA receptors. Figs. 2 and 3 show how an initial non-zero GO signal in coincidence with a delayed target stimulus does not trigger any response, which is only present when both signals are active. When the GO stimulus set the membrane potential of the GO population higher than the NMDA threshold, the arrival of a presynaptic spike from the target will provoke a post-synaptic spike. To get this behavior related to non-NMDA channels and prevent the firing, the excitation connection of the GO stimulus is the one which includes a short time depression mechanism; otherwise, the time increasing firing rate of the GO stimulus will make the neuron fire. Fig. 3 shows how increasing the slope of the GO stimulus the target is reached faster, as original algorithm.

V. Hardware Results

This section shows the results obtained with the hardware setup. The hardware setup consists of three VLSI chips a dedicate hardware infrastructure to operate them [21-22]. The chips comprise a total of 4224 leaky IF neurons and 16384 analog AER synapses. Both the neural and synaptic circuits exhibit biologically plausible adaptation mechanisms (e.g. short-term depression, spike frequency adaptation, etc.). Please refer to [1] for detailed descriptions of the circuits implementing the neuron and synaptic models. Finally, the neurosetup is connected to the AER Node board [23] using AER. At the end of the architecture, the robotic platform is located. It is a small robotic arm with cheap DC motors (OWI brand and model 535) and five degrees of freedom. One chip is used for each population: DV, GO and PPC. This division has been done on behalf of a better parameter tuning; otherwise, it will be not possible to achieve an accurate performance due to shared parameter among different populations. The number of neurons will depend on the robotic platform to control: when Pulse Frequency Modulation (PFM) is used, the firing rates to drive the motors will be fixed by the motor model. Thus, the number of neurons is fixed by the required firing rate. With this technique, the spikes can be supplied to the motors by spreading them the appropriate time length to avoid them to be filter by the motor and also a jerk movement (a jerk movement is a non-smooth one as the ancient 'robot' motion). For instance, if the rate is very small and the motor has a slow response, the spikes will be filtered and if we spread them too much, a jerk movement will be produced. So, a trade-off should be reached.

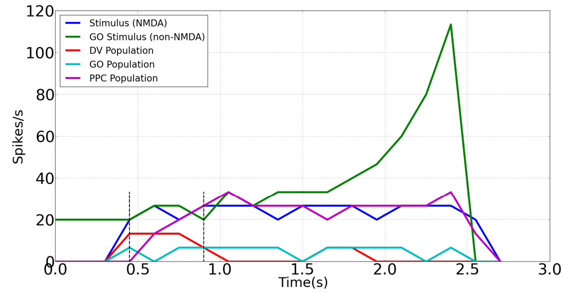

Fig. 2. Firing rates of one neuron of each population. The target stimulus is 25 spikes /s. Rates of the stimuli, DV population, GO population and PPC population are shown according to the legend. The PPC population reaches the target stimulus set in 0.45 seconds since its activation as is shown by the vertical dotted lines. Once the target is reached, the DV population is fully inhibited and if the stimulus is not supplied, the network activity does not produce any spiking activity.

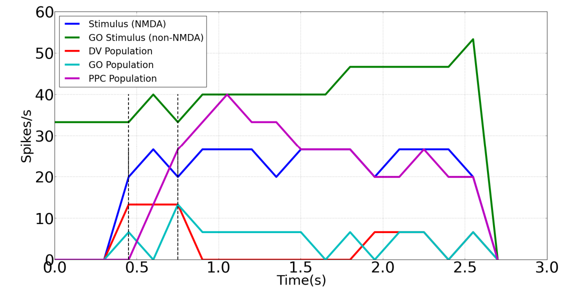

Fig. 3. Firing rates of one neuron of each population. The target stimulus is the same at the previous plot, 25 spikes / s but the slope profile is higher than the previous one and now, the target is reached in 0.3 seconds since its activation. Once the target is reached, the DV population is fully inhibited and if the stimulus is not supplied, the network activity does not produce any spiking activity.

Specifically, for this robotic model, the number of neurons per population needed to achieve a smooth control of the robotic arm was 60 IF neurons. The fashion connection is one-to-one. It results in a 60 replicated layers of the network showed in Fig.1 without any connection between them (that is the reason why only one neuron per population was used for the simulations). Fig. 4 shows the response of the hardware neural network which exhibits the same behavior observed in Fig. 2 (simulated network). Also, in this case, no spike is fired before the input stimulus is present. The implementation of the co-activation NMDA and non-NMDA is done using an excitatory connection with short time depression and the synapse implemented on the chip which includes the NMDA behavior. If the slope profile of the go stimulus is changed, Fig. 5 shows how the target is reached faster than the previous one keeping the input target with the same value and the same configuration for the population. The output activity of the PPC population is delivered to the FPGA to spread the spikes and eventually, drive the motor.

VI. Discussion

We proposed a novel model for motor control based on the work presented in [10]. The main difference with the previous model is that the response at the output of the GO multiplication is not a bell-shaped speed profile as it was stated in [10]. However, the functionality of the GO signal was not changed: the higher its slope, the faster the reaching movement. If we would try to recover the bell-shape profile for the output rate of GO population the dynamic response of the network will be driven by the GO stimulus and also the co-activation of the movement within the NMDA channels will be lost.

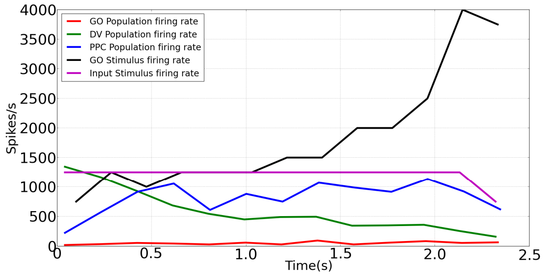

Fig. 4. Firing rates of each population implemented on the chips. The PPC population reaches the target stimulus set within 2 seconds. The input rate is 25 spikes / s. The plot shows the average firing rate of the whole population.

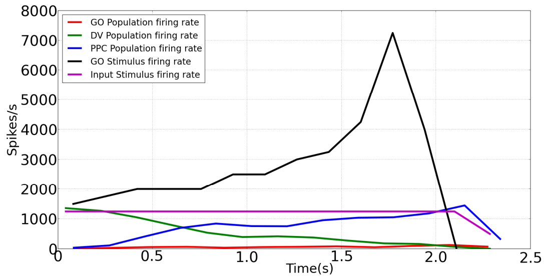

Fig. 5. Firing rates of each population. The slope profile is higher than the previous one and the target is reached in 1.8 seconds.

The approach presented has some important features: using PFM allows tuning of the duration of the spikes. This supports minimization of the effect of noisy spikes: a few randomly produced spikes cannot produce movements and are filtered by the motor. Furthermore, using VLSI IF chips give the possibility of tune many parameters; so, in principle, this model can be used for any robotic platform just changing the biases to adapt to the new desired features. However, if we aim to reduce the number of neurons of each population to be able to replicate the controller, a fast response DC motor should be driven to reduce the number of spikes needed.

The strongest link with biology is bound to the co-activation of the NMDA and non-NMDA channels (it was not present in the approach presented in [11]). The main con of this model is the open loop controller. This issue is now being solved by using DC motors that include sensory information as encoders. However, the open loop controller using the output rate of the PPC population within this configuration is quite interesting as far as the population has a temporal rate. This approach aims to set the basis for a full trajectory and stiffness neuro-inspired controller.

Acknowledgment

This work was supported by a grant from the German Academic Exchange Service (DAAD). Also, this work was supported by the Spanish grant (with support from the European Regional Development Fund) BIOSENSE (TEC2012-37868-C04-02/01) and the DFG funded Excellence Cluster 227 (CITEC, University of Bielefeld).

References

[1] E. Chicca, F. Stefanini, C. Bartolozzi, and G. Indiveri, "Neuromorphic Electronic Circuits for Building Autonomous Cognitive Systems," Proceedings of the IEEE, vol. pp, no. 99, pp. 1-22, May 2014.

[2] G. Indiveri, et al., "Neuromorphic silicon neuron circuits," Frontiers in Neuroscience, vol. 5, May 2011.

[3] J. Schemmel, et al., "Live demonstration: A scaled-down version of the BrainScaleS wafer-scale neuromorphic system," in International Symposium on Circuits and Systems. IEEE, 2012, pp. 702–702.

[4] B. V. Benjamin, et al. "Neurogrid: A Mixed-Analog-Digital Multichip System for Large-Scale Neural Simulations," Proceedings of the IEEE, vol. 102, no. 5, pp. 699,716, May 2014.

[5] S. B. Furber, F. Galluppi, S. Temple, and L.A. Plana, "The SpiNNaker Project," Proceedings of the IEEE, vol.102, no. 5, pp. 652-665, May 2014.

[6] C. Denk, et al., "Real-Time Interface Board for Closed-Loop Robotic Tasks on the SpiNNaker Neural Computing System," In International Conf. on Artificial Neural Networks, September 2013, pp. 467-474.

[7] A. Jimenez-Fernandez, et al., "A Neuro-Inspired Spike-Based PID Motor Controller for Multi-Motor Robots with Low Cost FPGAs," Sensors, vol. 12, no. 4, pp. 3831-3856, March 2012.

[8] S. Menon, S. Fok, A. Neckar, O. Khatib, and K. Boahen,"Controlling Articulated Robots in Task-Space with Spiking Silicon Neurons," Proceedings of the IEEE International Conference on Biomedical Robotics and Biomechatronics, August 2014

[9] P. Cisek, "Neural representations of motor plans, desired trajectories, and controlled objects," Cognitive Processing, vol. 6, no. 1, pp. 15-24, February 2005.

[10] D. Bullock and S. Grossberg, "Neural dynamics of planned arm movements: Emergent invariants and speed-accuracy properties during trajectory formation," Psychol Rev., vol. 95, pp. 49-90, January 1988.

[11] F. Perez-Peña, et al., "Neuro-Inspired Spike-Based Motion: From Dynamic Vision Sensor to Robot Motor Open-Loop Control through Spike-VITE," Sensors, vol. 13, pp. 15805-15832, November 2013.

[12] U. Pattacini, F. Nori, L. Natale, G. Metta and G. Sandini, "An experimental evaluation of a novel minimum-jerk cartesian controller for humanoid robots," in Intelligent Robots and Systems (IROS), IEEE/RSJ International Conference on, October 2010, pp. 1668 - 1674.

[13] A. Linares-Barranco, et al., "AER neuro-inspired interface to anthropomorphic robotic hand," in IEEE International Joint Conference on Neural Networks, July 2006, pp. 1497-1504.

[14] M. Hersch and A. G. Billard, "A biologically-inspired controller for reaching movements," Proceedings of the IEEE International Conference on Biomedical Robotics and Biomechatronics, pp. 1067-1072, February 2006.

[15] H. Mushiake and P. L. Strick, "Pallidal neuron activity during sequential arm movements," Journal of Neurophysiology, vol. 74, no. 6, pp. 2754–2758, December 1995.

[16] A. C. Guyton and J.E. Hall, Textbook of Medical Physiology. 11th ed. University of Michigan: Elsevier Saunders.

[17] M. L. Latash, Fundamentals of motor control, Elsevier, 2012.

[18] H. J. Groenewegen, "The basal ganglia and motor control," Neural Plasticity, vol. 10, no. 1-2, pp. 107–120, 2003.

[19] M. H. Qiu, M. C. Chen, Z. L. Huang, and J. Lu, "Neuronal activity (c-Fos) delineating interactions of the cerebral cortex and basal ganglia," Frontiers in Neuroanatomy, vol. 8, no. 13, March 2014.

[20] The Brian spiking neural network simulator. Available online: http://briansimulator.org/ (accessed on 20 March 2014).

[21] D. B. Fasnacht and G. Indiveri, "A PCI based high-fanout AER mapper with 2 GiB RAM look-up table, 0.8 µs latency and 66MHz output event-rate," Information Sciences and Systems (CISS), 2011 45th Annual Conference on, pp.1-6, March 2011.

[22] D.B. Fasnacht, A.M. Whatley, and G. Indiveri, "A Serial Communication Infrastructure for Multi-Chip Address Event System," in International Symposium on Circuits and Systems. IEEE, May 2008, pp. 648-651.

[23] T. Iakymchuk, et al. "An AER Handshake-Less Modular Infraestructure PCB with x8 2.5Gbps LVDS Serial Links," in International Symposium on Circuits and Systems. IEEE, June 2014.